Available online at www.sciencedirect.com
ScienceDirect
European Journal of Medicinal Chemistry 44 (2009) 359–364
EUROPEAN JOURNAL OF MEDICINAL CHEMISTRY
http://www.elsevier.com/locate/ejmech

Original article

QSAR modelling of pancreatic β-cell K_{ATP} channel openers *R*/*S*-3,4-dihydro-2,2-dimethyl-6-halo-4-(substituted phenylaminocarbonylamino)-2*H*-1-benzopyrans using MLR–FA techniques

Sk. Mahasin Alam, Soma Samanta, Amit Kumar Halder, Soumya Basu, Tarun Jha*

Medicinal and Pharmaceutical Chemistry, Department of Pharmaceutical Technology, P.O. Box 17020, Jadavpur University, Kolkata 700 032, West Bengal, India

Received 17 July 2007; received in revised form 25 January 2008; accepted 29 February 2008
Available online 12 March 2008

Abstract

Potassium (K^+) channel openers are a diverse group of compounds which are used for the treatment of diseases like angina pectoris, hypertension, congestive heart failure, anti-hypoglycemic (insulinoma), bronchial asthma, etc. *R*/*S*-3,4-dihydro-2,2-dimethyl-6-halo-4-(substituted phenylaminocarbonylamino)-2*H*-1-benzopyrans are a new series of ATP-sensitive potassium ($K_{ATP\text{-}p\beta}$) channel openers selective towards pancreatic β-cells. QSAR modelling was done on these series of compounds to find a more active and selective $K_{ATP\text{-}p\beta}$ channel opener selective towards β-cells of pancreatic tissues. Wang–Ford charges, partition coefficient, molar refractivity, principle moment of inertia at *X*, *Y* and *Z* axes are used as predictor variables and logarithm of percentage of residual insulin secretion is treated as response variable for the modelling. Multiple linear regressions with factor analysis were performed to develop QSAR models. Four equations were obtained using different combinations of the predictor variables based on factor loadings. Regression coefficients of all descriptors used are significant at more than 95% level. Results showed that Wang–Ford charges on atom numbers 11, 17, 18, 19 and 21 are important for the inhibition of residual insulin secretion. The presence of electron withdrawing group at *m*- and *p*-position of phenyl ring B is required for the inhibition. The energy minimized geometry of the most active compound supported our modelling.

Keywords: Potassium channel openers; Benzopyran derivatives; Wang–Ford charges; MLR–FA; QSAR modelling

1. Introduction

Potassium (K^+) channels are of different types e.g., voltage dependent, Ca^{2+} activated, receptor operated, ATP sensitive, Na^+ activated and cell volume sensitive. Activation of K^+ channel results in outflow of K^+ ions and leads to the hyperpolarization of the cell membrane [1,2]. Potassium (K^+) channel openers (PCOs) are a diverse group of compounds. These exert their effects on the secretory cells, neurons, vascular and non-vascular smooth muscles and cardiac skeletal muscle by opening ATP-sensitive potassium (K_{ATP}) channels. ATP-sensitive K^+ (K_{ATP}) channels are composed of pore forming inwardly rectifying potassium channel subunits and regulatory sulfonylurea receptor subunits, SURs [3]. K_{ATP} channels are distributed in a wide variety of tissues like skeletal and smooth muscle cells, cardiac myocytes and neurons. K_{ATP} channels are activated by drugs like minoxidil, diazoxide, pinacidil and benzopyran derivatives e.g., cromakalim, bimakalim, etc. [4]. K_{ATP} channel activation antagonizes the action of intracellular ATP on these channels, thus, open these and causes the hyperpolarization which relaxes smooth muscle and promotes the inhibition of endocrine and/or neurotransmitter release [5,6]. PCOs are used for the treatment of diseases like angina pectoris, hypertension, congestive heart failure, myocardial salvage in

* Corresponding author. Tel.: +91 33 24146666x2495 (o), +91 33 24383814 (r), 09433187443 (m); fax: +91 33 24146927.
E-mail address: tjupharm@yahoo.com (T. Jha).

0223-5234/$ - see front matter © 2008 Elsevier Masson SAS. All rights reserved.
doi:10.1016/j.ejmech.2008.02.042

myocardial infarction (MI), anti-hypoglycemia (insulinoma), alopecia, bronchial asthma, urinary urge incontinence, Raynaud's disease, etc. [7]. 4,6-Disubstituted 2,2-dimethyl chromans, structurally related to cromakalim, were synthesized and pharmacologically evaluated for the selective inhibition of insulin secretion by Sebille et al. [8]. These derivatives are active and selective K_{ATP} channel openers of pancreatic tissues ($K_{ATP\text{-}p\beta}$) and are inhibitors of insulin secretion [8].

As a part of our composite program of rational drug design [9–13], a quantitative structure activity relationship (QSAR) modelling was performed on *R*/*S*-3,4-dihydro-2,2-dimethyl-6-halo-4-(substituted phenylaminocarbonylamino)-2*H*-1-benzopyrans to find a more active and selective potassium ($K_{ATP\text{-}p\beta}$) channel opener for the pancreatic tissues. The general structure of *R*/*S*-3,4-dihydro-2,2-dimethyl-6-halo-4-(substituted phenylaminocarbonylamino)-2*H*-1-benzopyrans with arbitrary numbering is shown in Fig. 1.

2. Materials and methods

Dataset, parameters and different statistical methods used to develop statistically significant QSAR models are described in the following sections.

2.1. Dataset and parameters

Percentage of residual insulin secretion data of *R*/*S*-3,4-dihydro-2,2-dimethyl-6-halo-4-(substituted phenylaminocarbonylamino)-2*H*-1-benzopyrans was collected from the published work of Sebille et al. [8]. For the measurement of insulin secretion, isolated pancreatic islets from rats were used by these groups [8]. Insulin release was measured radio-immunologically and expressed in terms of percentage of residual insulin secretion (PRIS). Compounds which have lower PRIS value are highly active as potassium ($K_{ATP\text{-}p\beta}$) channel openers and inhibit insulin secretion. Logarithm of percentage residual insulin secretion (log PRIS) was computed and taken as the response variable for QSAR modelling and is listed in Table 1.

Semi-empirical quantum chemical descriptors (Wang–Ford charges – q_x), partition coefficient (log *P*), molar refractivity (MR), the principle moment of inertia (PMX, PMY and PMZ) and indicator parameters are used as the predictor variables. Wang–Ford charges (q_x), partition coefficient (log *P*), molar refractivity (MR) and the principle moment of inertia

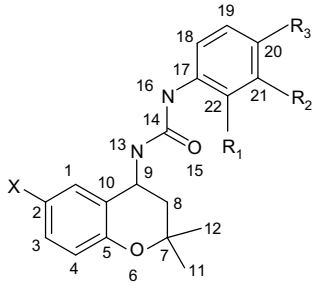

Fig. 1. General structure of *R*/*S*-3,4-dihydro-2,2-dimethyl-6-halo-4-(substituted phenylaminocarbonylamino)-2*H*-1-benzopyrans with arbitrary numbering.

Table 1
Percentage residual insulin secretion of *R*/*S*-3,4-dihydro-2,2-dimethyl-6-halo-4-(substituted phenylaminocarbonylamino)-2*H*-1-benzopyrans

Compound number	X	R_1	R_2	R_3	PRIS[a]	log PRIS
1	F	H	H	H	83.8 ± 3.5	1.923
2	Cl	H	H	H	87.7 ± 3.5	1.943
3	Br	H	H	H	75.9 ± 4.0	1.880
4	F	OCH_3	H	H	88.4 ± 4.8	1.946
5	Cl	OCH_3	H	H	94.6 ± 3.7	1.976
6	Br	OCH_3	H	H	72.8 ± 5.5	1.862
7	F	H	OCH_3	H	66.6 ± 3.3	1.823
8	Cl	H	OCH_3	H	84.0 ± 4.8	1.924
9	Br	H	OCH_3	H	73.5 ± 4.0	1.866
10	F	H	H	OCH_3	89.0 ± 3.9	1.949
11	Cl	H	H	OCH_3	79.3 ± 4.6	1.899
12	Br	H	H	OCH_3	79.2 ± 3.7	1.899
13	F	CH_3	H	H	79.0 ± 3.3	1.898
14	Cl	CH_3	H	H	85.0 ± 3.1	1.929
15	Br	CH_3	H	H	79.5 ± 3.5	1.900
16	F	H	CH_3	H	75.2 ± 2.7	1.876
17	Cl	H	CH_3	H	65.8 ± 4.4	1.818
18	Br	H	CH_3	H	63.4 ± 3.1	1.802
19	F	H	H	CH_3	70.6 ± 3.8	1.849
20	Cl	H	H	CH_3	69.5 ± 3.4	1.842
21	Br	H	H	CH_3	72.9 ± 4.0	1.863
22	F	Cl	H	H	51.4 ± 3.1	1.711
23	Cl	Cl	H	H	40.3 ± 1.5	1.605
24	Br	Cl	H	H	41.8 ± 3.5	1.621
25	F	H	Cl	H	28.0 ± 1.5	1.447
26	Cl	H	Cl	H	25.0 ± 1.3	1.398
27	Br	H	Cl	H	28.6 ± 1.7	1.456
28	F	H	H	Cl	22.8 ± 1.2	1.358
29	Cl	H	H	Cl	34.6 ± 1.9	1.539
30	Br	H	H	Cl	25.7 ± 1.5	1.410

[a] PRIS indicates the percentage of residual insulin secretion (mean ± SEM).

(PMX, PMY and PMZ) were calculated using *Chem3D Pro* package [14]. The hydrogen-suppressed geometry of compounds was used for the calculation of q_x, log *P*, MR, PMX, PMY and PMZ. The 2D model of compounds was drawn in ChemDraw Ultra and converted in 3D model in Chem3D Pro. Energy minimization was done under MOPAC module according to AM1 (Austin Model 1) method using RHF (restricted Hartree–Fock: closed shell) wave function. Wang–Ford charges (q_x) were calculated using energy-minimized geometry. log *P* and MR were calculated based on Ghose and Crippen's fragmentation method. Indicator parameters were also used to find out the role of the specific substituent at the specific position(s) towards the activity.

2.2. Statistical analysis

Different statistical methods used to develop QSAR models are described as follows.

2.2.1. Cluster analysis

k-Mean cluster analysis was performed to design training and test set. A k-MCA split the compounds into four clusters with 13, 1, 12, and 4 members. 25% members were selected randomly from each cluster for designing the test set.

Remaining set of compounds were treated as the training set. QSAR models were developed using the training set.

2.2.2. Factor analysis

Factor analysis (FA) [15] was carried out as the pre-processing step of data for the variable selection on the training set containing the response variable and all descriptors. Principal component method was employed to extract the factors and then rotated by VARIMAX (variance maximizing) rotation. The goal of VARIMAX rotation is to maximize the variance of the new variable (factor) while minimizing the variance around the new variable. Factor loadings of different variables are listed in Table 2. Seven factors were extracted. Factor loadings more than 0.7 are shown in bold face.

2.2.3. Multiple linear regressions

Multiple linear regression (MLR) analysis [16] was used to develop QSAR models. Different combinations of parameters (factor loadings more than 0.7) belonging to different factors were tried to develop these models. Correlation analysis was carried out on these selected parameters. Intercorrelated parameters were eliminated. Statistical qualities of MLR equations were judged by parameters like correlation coefficient (R), adjusted R^2 (R^2_a), variance ratio (F), probability factor related to F-ratio (p) and standard error of estimate (s).

2.2.4. Validation of QSAR models

Leave-one-out (LOO) cross validation method was used to validate the developed QSAR models. By using this, the predictive powers of equations were validated. Predicted residual sum of square (PRESS), total sum of squares (SSY), cross-validated R^2 (R^2_{cv}), standard deviation error of prediction (SDEP) and standard error of PRESS (S_{PRESS}) were considered for validation of these models.

2.2.5. Prediction of test set compounds

On the basis of the developed QSAR models the activities of the test set compounds were predicted and R^2_{Pred} values for the test set were calculated.

3. Results and discussion

On the basis of k-mean cluster analysis, twenty three compounds among thirty compounds were selected as the training set and remaining seven compounds (compound numbers **2**, **8**, **14**, **21**, **22**, **26** and **30**) were selected as the test set. Factor analysis was performed on the training set. Combinations of parameters which have factor loadings more than 0.7 were considered for the multiple linear regression analysis. The selected parameters used to develop the QSAR models are

Table 2
Factor loadings of the variables after VARIMAX rotation

Descriptors	F1[a]	F2[a]	F3[a]	F4[a]	F5[a]	F6[a]	F7[a]	Communality[b]
log PRIS	0.033	0.300	0.263	−0.166	−0.694	0.113	0.484	0.917
q_1	**0.974**	−0.014	−0.126	0.026	0.033	−0.014	−0.067	0.971
q_2	**−0.974**	−0.100	0.080	−0.032	−0.043	0.108	−0.024	0.979
q_3	**0.974**	0.112	−0.064	0.041	0.023	−0.111	0.035	0.980
q_4	**−0.982**	−0.053	0.012	0.009	0.069	0.083	−0.007	0.979
q_5	**0.912**	−0.212	0.061	0.142	−0.253	0.107	−0.022	0.976
q_6	−0.026	0.408	−0.127	−0.341	**0.799**	−0.111	−0.151	0.974
q_7	−0.316	−0.313	0.158	0.552	−0.641	0.030	0.196	0.978
q_8	0.228	0.274	−0.601	−0.246	0.613	−0.009	0.001	0.925
q_9	−0.353	−0.281	0.449	−0.608	−0.071	0.318	−0.180	0.914
q_{10}	−0.398	0.490	−0.082	0.362	0.004	−0.427	0.387	0.868
q_{11}	0.176	0.154	0.000	**−0.931**	0.211	−0.034	0.013	0.967
q_{12}	−0.103	−0.051	0.278	0.331	**−0.797**	−0.199	−0.141	0.894
q_{13}	0.249	0.376	0.207	**0.709**	0.164	−0.292	−0.037	0.862
q_{14}	−0.173	**−0.853**	−0.146	−0.055	−0.061	0.053	0.000	0.789
q_{15}	0.138	**0.813**	−0.309	−0.095	0.384	0.060	0.107	0.947
q_{16}	0.038	**0.816**	−0.439	0.250	0.112	0.178	0.103	0.977
q_{17}	0.032	**−0.951**	0.055	−0.148	0.007	−0.061	−0.067	0.939
q_{18}	0.016	**0.815**	0.531	−0.027	−0.056	0.078	0.132	0.974
q_{19}	0.002	−0.264	**−0.901**	−0.015	0.135	−0.116	−0.259	0.982
q_{20}	−0.031	−0.029	**0.886**	0.151	−0.120	0.335	0.091	0.945
q_{21}	0.088	−0.015	**−0.948**	0.094	0.059	0.139	−0.037	0.940
q_{22}	−0.034	**0.860**	0.275	−0.164	0.096	−0.255	0.016	0.917
log P	0.696	−0.437	−0.151	0.105	0.350	−0.225	−0.047	0.884
MR	**0.887**	0.313	0.034	0.084	0.072	0.045	0.027	0.902
PMX	**0.738**	0.048	−0.033	−0.283	0.442	−0.079	0.139	0.850
PMY	−0.242	0.047	0.166	0.033	−0.048	**0.844**	0.054	0.807
PMZ	0.239	0.117	−0.012	**0.899**	−0.103	0.195	−0.096	0.937
I_ClR_2	−0.146	0.043	0.170	0.395	**0.858**	−0.135	0.085	0.969
I_ClR_3	−0.065	−0.139	−0.240	0.029	0.034	−0.030	**−0.941**	0.969
Variance	0.241	0.192	0.142	0.127	0.134	0.054	0.054	0.930

Factor loadings more than 0.7 are shown in bold face.

[a] F1–7 represents the factor loading of the variables.

[b] Communality of a variable is the sum of squares of its loading in different factors.

listed in Table 3. From the factor analysis performed on data matrix consisting of the response variable and all descriptors, it was observed that seven factors could explain the data matrix to the extent of 93% (Table 2). The response variable (log PRIS) is highly loaded in factor 5 (highly loaded with q_6, q_{12} and I_ClR_2) and factor 7 (highly loaded with I_ClR_3), moderately loaded with factor 2 (highly loaded with q_{14}, q_{15}, q_{16}, q_{17}, q_{18} and q_{22}) and factor 3 (highly loaded with q_{19}, q_{20} and q_{21}) and poorly loaded with factor 4 (highly loaded q_{11}, q_{13} and PMZ), factor 6 (highly loaded with PMY) and factor 1 (highly loaded with q_1, q_2, q_3, q_4, q_5, MR and PMX). Following equations were obtained based on the factor analysis:

$$\log \mathrm{PRIS} = 2.001(\pm 0.042) + 0.730(\pm 0.189)q_{18} - 0.408(\pm 0.055)I\_ClR_2 - 0.326(\pm 0.059)I\_ClR_3 \quad (1)$$

$$n = 23,\ R = 0.926,\ R^2 = 0.857,\ R^2_A = 0.835,\ F_{(3,19)} = 38.099,\ p < 0.00001,\ s = 0.074,\ R^2_{cv} = 0.843,\ \mathrm{SSY} = 0.725,\ \mathrm{PRESS} = 0.171,\ \mathrm{SDEP} = 0.075,\ S_{\mathrm{PRESS}} = 0.081.$$

Table 3
Wang–Ford charges of different common atoms and indicator parameters

Compound number	q_{11} [a]	q_{17} [a]	q_{18} [a]	q_{19} [a]	q_{21} [a]	I_ClR_2 [b]	I_ClR_3 [b]
1	−0.373	0.363	−0.248	−0.030	−0.085	0	0
2	−0.376	0.349	−0.239	−0.033	−0.079	0	0
3	−0.368	0.360	−0.242	−0.037	−0.091	0	0
4	−0.239	0.081	−0.039	−0.207	−0.264	0	0
5	−0.246	0.095	−0.057	−0.194	−0.268	0	0
6	−0.249	0.126	−0.076	−0.180	−0.250	0	0
7	−0.358	0.231	−0.249	0.010	0.346	0	0
8	−0.365	0.214	−0.232	−0.001	0.344	0	0
9	−0.367	0.231	−0.241	0.003	0.345	0	0
10	−0.36	0.220	−0.109	−0.234	−0.205	0	0
11	−0.373	0.205	−0.100	−0.241	−0.204	0	0
12	−0.379	0.215	−0.098	−0.240	−0.203	0	0
13	−0.384	0.860	−0.287	−0.309	−0.551	0	0
14	−0.381	0.239	−0.163	−0.087	−0.124	0	0
15	−0.380	0.247	−0.170	−0.082	−0.119	0	0
16	−0.370	0.349	−0.258	−0.021	0.067	0	0
17	−0.371	0.343	−0.254	−0.024	0.070	0	0
18	−0.367	0.345	−0.254	−0.024	0.070	0	0
19	−0.259	0.422	−0.250	−0.052	−0.063	0	0
20	−0.286	0.437	−0.246	−0.050	−0.059	0	0
21	−0.272	0.455	−0.287	0.001	−0.044	0	0
22	−0.217	0.618	−0.298	−0.010	0.080	0	0
23	−0.226	0.621	−0.308	−0.009	0.061	0	0
24	−0.241	0.660	−0.339	0.010	0.087	0	0
25	−0.375	0.311	−0.202	−0.104	−0.121	1	0
26	−0.375	0.280	−0.176	−0.108	−0.164	1	0
27	−0.364	0.289	−0.187	−0.113	−0.122	1	0
28	−0.381	0.417	−0.324	0.142	0.067	0	1
29	−0.305	0.444	−0.299	0.066	0.114	0	1
30	−0.378	0.412	−0.319	0.141	0.072	0	1

[a] q_{11}, q_{17} q_{18}, q_{19} and q_{21} indicate the Wang–Ford charges of atom numbers 11, 17, 18, 19 and 21, respectively.

[b] I_ClR_2 indicates the presence or absence of chlorine atom at R_2 position and I_ClR_3 indicates the presence or absence of chlorine atom at R_3 position.

where n is the number of data point. The 95% confidence intervals of the regression coefficient are shown in parentheses. Eq. (1) explains 83.5% and predicts 84.3% of the variance of activity. This equation shows the importance of Wang–Ford charge of atom 18 (q_{18}) and the indicator parameters I_ClR_2 and I_ClR_3 for the inhibition of residual insulin secretion from pancreatic β-cells. The positive coefficient of q_{18} suggests that the higher negative charge on atom 18 is conducive for the inhibition of residual insulin secretion. I_ClR_2 indicates the presence or absence of chlorine atom at R_2 position while I_ClR_3 indicates the presence or absence of chlorine atom at R_3 position. The negative coefficients of I_ClR_2 and I_ClR_3 indicate that presence of chlorine atom at R_2 and R_3 positions of the general structure is favorable for the inhibition of residual insulin secretion.

Another model (Eq. (2)) was developed using Wang–Ford charges of atom numbers 17, 19 and indicator parameters.

$$\log \mathrm{PRIS} = 1.887(\pm 0.037) - 0.237(\pm 0.081)q_{17} - 0.477(\pm 0.152)q_{19} - 0.415(\pm 0.051)I\_ClR_2 - 0.286(\pm 0.059)I\_ClR_3$$

$$n = 23,\ R = 0.941,\ R^2 = 0.885,\ R^2_A = 0.859,\ F_{(4,18)} = 34.609,\ p < 0.00001,\ s = 0.068,\ R^2_{cv} = 0.805,\ \mathrm{SSY} = 0.725,\ \mathrm{PRESS} = 0.212,\ \mathrm{SDEP} = 0.084,\ S_{\mathrm{PRESS}} = 0.092. \quad (2)$$

Eq. (2) explains 85.9% and predicts 80.5% of the variance of activity. The negative coefficient of q_{17} indicates that the higher positive charge on atom 17 is conducive for the inhibition of residual insulin secretion while the negative coefficient of q_{19} indicates that the higher negative charge on atom 19 is detrimental for the inhibition of residual insulin secretion as decreased the value of PRIS indicates the inhibition of residual insulin secretion increased.

Replacement of q_{19} from Eq. (2) by q_{21} yielded an equally significant model (Eq. (3))

$$\log \mathrm{PRIS} = 1.938(\pm 0.032) - 0.295(\pm 0.081)q_{17} - 0.227(\pm 0.075)q_{21} - 0.426(\pm 0.052)I\_ClR_2 - 0.342(\pm 0.053)I\_ClR_3$$

$$n = 23,\ R = 0.939,\ R^2 = 0.882,\ R^2_A = 0.856,\ F_{(4,18)} = 33.595,\ p < 0.00001,\ s = 0.069,\ R^2_{cv} = 0.785,\ \mathrm{SSY} = 0.725,\ \mathrm{PRESS} = 0.234,\ \mathrm{SDEP} = 0.08,\ S_{\mathrm{PRESS}} = 0.097. \quad (3)$$

Eq. (3) explains 85.6% and predicts 78.5% of variance of the activity. The negative coefficient of q_{21} indicates that with the increase in negative charge on atom 21 the inhibition of residual insulin secretion decreases.

Combination of q_{11} in Eq. (3) yielded a different model shown in Eq. (4).

Table 4
Correlation matrix for response variable, Wang–Ford charges and indicator parameters

	log PRIS	q_{11}	q_{17}	q_{18}	q_{19}	q_{21}	I_ClR_2	I_ClR_3
log PRIS	1.00	0.03	−0.32	0.51	−0.54	−0.31	−0.58	−0.58
q_{11}		1.00	0.02	0.13	0.00	−0.06	−0.21	−0.06
q_{17}			1.00	−0.79	0.21	−0.03	−0.07	0.15
q_{18}				1.00	−0.73	−0.53	0.06	−0.36
q_{19}					1.00	0.83	−0.07	0.52
q_{21}						1.00	−0.10	0.23
I_ClR_2							1.00	−0.10
I_ClR_3								1.00

$$\log \mathrm{PRIS} = 1.769(\pm 0.083) - 0.515(\pm 0.236)q_{11} - 0.292(\pm 0.074)q_{17} - 0.237(\pm 0.069)q_{21} - 0.448(\pm 0.048)I\_ClR_2 - 0.350(\pm 0.049)I\_ClR_2$$
$$n = 23,\ R = 0.953,\ R^2 = 0.908,\ R^2_A = 0.881,\ F_{(5,17)} = 33.452,\ p < 0.00001,\ s = 0.063,\ R^2_{cv} = 0.795,\ \mathrm{SSY} = 0.725,\ \mathrm{PRESS} = 0.223,\ \mathrm{SDEP} = 0.086,\ S_{\mathrm{PRESS}} = 0.096. \quad (4)$$

Eq. (4) explains 88.1% and predicts 79.5% of the variance of activity. The negative coefficient of q_{11} indicates that the higher negative charge on atom 11 is detrimental for the inhibition of residual insulin secretion.

The correlation matrix among the response variable and descriptors used in Eqs. (1)–(4) is listed in Table 4. The observed (Obs), calculated (Calc), residual (Res), predicted residual (Pres) and LOO-predicted (Pred) activities of Eqs. (1)–(4) are shown in Tables 5a and 5b. All coefficients of parameters and intercepts in all equations are of 95% confidence intervals as supported by their *t*- and *p*-values. The *t*- and *p*-values of Eqs. (1)–(4) are shown in Table 6. In Eqs. (1)–(4), the recommended ratio of number of predictor parameters to number of data point of 1:5 was maintained [17,18].

Table 5a
Observed (Obs), calculated (Calc), residual (Res), predicted residual (Pres) and LOO-predicted (Pred) activities of Eqs. (1) and (2)

Compound number	Obs	Eq. (1)				Eq. (2)			
		Calc	Res	Pres	Pred	Calc	Res	Pres	Pred
1	1.923	1.821	0.103	0.110	1.813	1.815	0.108	0.117	1.806
3	1.880	1.825	0.055	0.059	1.821	1.819	0.061	0.066	1.814
4	1.946	1.973	−0.027	−0.034	1.981	1.966	−0.020	−0.024	1.970
5	1.976	1.960	0.016	0.020	1.956	1.957	0.019	0.023	1.953
6	1.862	1.946	−0.084	−0.099	1.961	1.943	−0.080	−0.093	1.955
7	1.823	1.820	0.004	0.004	1.820	1.827	−0.004	−0.004	1.828
9	1.866	1.826	0.041	0.043	1.823	1.830	0.036	0.041	1.825
10	1.949	1.922	0.027	0.031	1.919	1.946	0.003	0.004	1.945
11	1.899	1.929	−0.029	−0.033	1.932	1.953	−0.054	−0.064	1.963
12	1.899	1.930	−0.031	−0.036	1.934	1.950	−0.051	−0.061	1.960
13	1.898	1.792	0.106	0.117	1.780	1.830	0.068	0.266	1.632
15	1.900	1.877	0.023	0.024	1.876	1.867	0.033	0.036	1.865
16	1.876	1.813	0.063	0.068	1.808	1.814	0.062	0.068	1.808
17	1.818	1.816	0.002	0.002	1.816	1.817	0.001	0.002	1.817
18	1.802	1.816	−0.014	−0.015	1.817	1.816	−0.014	−0.015	1.818
19	1.849	1.819	0.030	0.032	1.817	1.811	0.037	0.040	1.808
20	1.842	1.822	0.020	0.021	1.821	1.807	0.035	0.038	1.804
23	1.605	1.777	−0.171	−0.196	1.802	1.744	−0.138	−0.170	1.775
24	1.621	1.754	−0.133	−0.162	1.783	1.725	−0.104	−0.136	1.757
25	1.447	1.446	0.001	0.002	1.445	1.447	0.000	0.000	1.447
27	1.456	1.457	−0.001	−0.002	1.458	1.457	0.000	0.000	1.457
28	1.358	1.439	−0.081	−0.163	1.521	1.434	−0.076	−0.154	1.512
29	1.539	1.458	0.081	0.163	1.376	1.463	0.076	0.154	1.385

Table 5b
Observed (Obs), calculated (Calc), residual (Res), predicted residual (Pres) and LOO-predicted (Pred) activities of Eqs. (3) and (4)

Compound number	Obs	Eq. (3)				Eq. (4)			
		Calc	Res	Pres	Pred	Calc	Res	Pres	Pred
1	1.923	1.851	0.073	0.077	1.774	1.875	0.048	0.053	1.870
3	1.880	1.853	0.027	0.029	1.824	1.875	0.006	0.006	1.874
4	1.946	1.974	−0.028	−0.035	2.009	1.931	0.016	0.022	1.924
5	1.976	1.971	0.005	0.006	1.965	1.931	0.045	0.062	1.914
6	1.862	1.958	−0.096	−0.114	2.072	1.919	−0.057	−0.075	1.938
7	1.823	1.791	0.032	0.044	1.748	1.804	0.020	0.027	1.796
9	1.866	1.792	0.075	0.101	1.690	1.809	0.058	0.080	1.786
10	1.949	1.920	0.029	0.032	1.888	1.939	0.011	0.012	1.937
11	1.899	1.924	−0.025	−0.028	1.952	1.949	−0.050	−0.058	1.957
12	1.899	1.921	−0.022	−0.025	1.946	1.949	−0.051	−0.059	1.958
13	1.898	1.810	0.087	0.258	1.552	1.846	0.052	0.191	1.706
15	1.900	1.893	0.008	0.008	1.884	1.921	−0.020	−0.023	1.923
16	1.876	1.820	0.056	0.061	1.760	1.842	0.035	0.039	1.838
17	1.818	1.821	−0.003	−0.003	1.825	1.843	−0.025	−0.028	1.846
18	1.802	1.821	−0.019	−0.020	1.841	1.840	−0.038	−0.042	1.845
19	1.849	1.828	0.021	0.022	1.806	1.794	0.055	0.063	1.786
20	1.842	1.823	0.019	0.020	1.802	1.802	0.040	0.043	1.798
23	1.605	1.741	−0.136	−0.168	1.910	1.689	−0.084	−0.127	1.732
24	1.621	1.724	−0.103	−0.135	1.859	1.679	−0.058	−0.088	1.710
25	1.447	1.448	−0.001	−0.003	1.451	1.451	−0.004	−0.008	1.455
27	1.456	1.455	0.001	0.003	1.453	1.452	0.004	0.008	1.448
28	1.358	1.458	−0.100	−0.200	1.658	1.478	−0.120	−0.250	1.608
29	1.539	1.439	0.100	0.200	1.239	1.419	0.120	0.250	1.289

Table 6
The *t*- and *p*-values of Eqs. (1)–(4)

Equation number	Intercepts/parameters	*t*-Value	*p*-Value
(1)	Intercept	48.066	0.000
	q_{18}	3.861	0.001
	I_ClR_3	−7.437	0.000
	I_ClR_2	−5.554	0.000
(2)	Intercept	51.262	0.000
	q_{17}	−2.928	0.009
	q_{19}	−3.139	0.007
	I_ClR_3	−8.195	0.000
	I_ClR_2	−4.833	0.000
(3)	Intercept	60.993	0.000
	q_{17}	−3.622	0.002
	q_{21}	−3.021	0.007
	I_ClR_2	−8.261	0.000
	I_ClR_3	−6.419	0.000
(4)	Intercept	21.358	0.000
	q_{11}	−2.183	0.043
	q_{17}	−3.952	0.001
	q_{21}	−3.454	0.003
	I_ClR_2	−9.342	0.000
	I_ClR_3	−7.193	0.000

Table 7
Observed and predicted values of the test set compounds

Compound number	Obs	Pred value			
		Eq. (1)	Eq. (2)	Eq. (3)	Eq. (4)
2	1.943	1.827	1.82	1.853	1.879
8	1.924	1.832	1.836	1.797	1.813
22	1.711	1.784	1.745	1.738	1.681
14	1.929	1.883	1.871	1.896	1.925
21	1.863	1.792	1.778	1.814	1.786
26	1.398	1.465	1.456	1.467	1.471
30	1.410	1.443	1.435	1.458	1.476
R^2_{Pred}		0.891	0.895	0.903	0.910

Predicted values of the test set compounds were calculated on the basis of Eqs. (1)–(4). The observed and predicted values of the test set compounds are listed in Table 7. Significant R^2_{Pred} values for the test set were obtained and shown as follows:

$R^2_{\text{Pred}} = 0.891$ for Eq. (1).
$R^2_{\text{Pred}} = 0.895$ for Eq. (2).
$R^2_{\text{Pred}} = 0.903$ for Eq. (3).
$R^2_{\text{Pred}} = 0.910$ for Eq. (4).

4. Conclusion

The present study suggests the importance of Wang–Ford charges on atom numbers 11, 17, 18, 19 and 21 of the general structure for the inhibition of residual insulin secretion. From the signs of regression coefficients, it is evident that increase in negative charge on atom 18 is favorable for the inhibition of residual insulin secretion while increase in positive charge on atom 17 is favorable for the inhibition. The results also show that increase in the negative charges on atoms 11, 19 and 21 are unfavorable for the inhibition of residual insulin secretion. The electron-withdrawing substituents at *m*-(R_2) and *p*-(R_3) position of phenyl ring B (Fig. 1) are required for the inhibition of residual insulin secretion. The energy-minimized geometry of the most active compound (compound **28**) supported our modelling and is presented in Fig. 2.

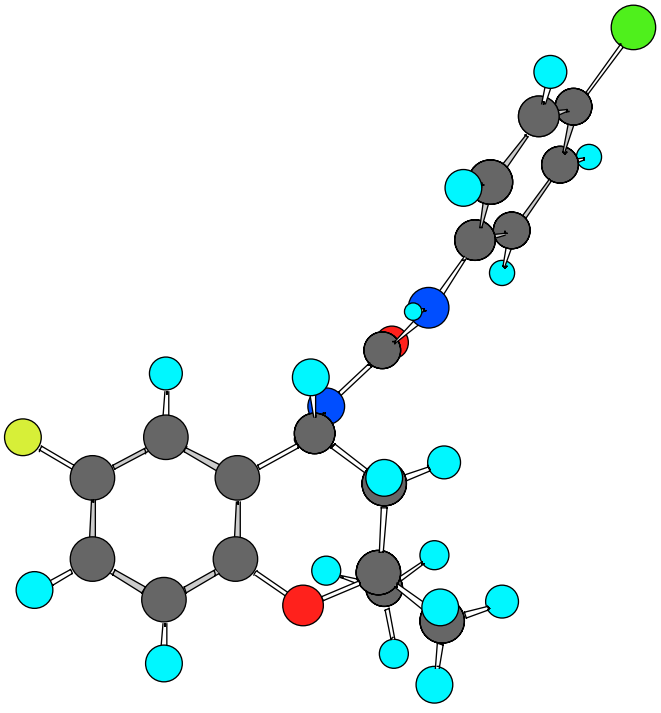

Fig. 2. The energy-minimized geometry of the most active compound (compound **28**).

Acknowledgements

The authors are grateful to All India Council for Technical Education (AICTE), New Delhi and University Grants Commission (UGC), New Delhi for awarding research projects. One of the authors (S.S.) is thankful to UGC for providing a Senior Research Fellowship (SRF). Authors are also grateful to the authority of Jadavpur University for their help and encouragement.

References

[1] M. Gopalakrishnan, C.C. Shieh, Expert Opin. Ther. Targets 8 (2004) 437–458.
[2] A. Szewczyk, J. Skalska, M. Glab, B. Kulawiak, D. Malinska, I. Koszela-Piotrowska, W.S. Kunz, Mitochondrial potassium channels: from pharmacology to function, Biochim. Biophys. Acta 1757 (2006) 715–720.
[3] M. Schwanstecher, C. Sieverding, H. Dorschner, I. Gross, L. Aguilar-Bryan, C. Schwanstecher, J. Bryan, EMBO J. 17 (1998) 5529–5535.
[4] J.R. Fozard, P.W. Manley, Prog. Respir. Res. 31 (2001) 77–80.
[5] H.P. Rang, M.M. Dale, J.M. Ritter, P.K. Moore, Pharmacology, Churchill Livingstone, Edinburgh, 2003.
[6] K. Lawson, Pharmacol. Ther. 70 (1996) 39–63.
[7] K.D. Tripathi, Essentials of Medical Pharmacology, Jaypee Brothers Medical Publishers Ltd., New Delhi, 2003.
[8] S. Sebille, D. Gall, P. de Tullio, X. Florence, P. Lebrun, B. Pirotte, J. Med. Chem. 49 (2006) 4690–4697.
[9] S. Samanta, B. Debnath, S. Gayen, B. Ghosh, K. Srikanth, T. Jha, Farmaco 60 (2005) 818–825.
[10] S. Samanta, B. Debnath, A. Basu, S. Gayen, K. Srikanth, T. Jha, Eur. J. Med. Chem. 41 (2006) 1190–1195.
[11] S. Samanta, Sk. M. Alam, P. Panda, T. Jha, Internet Electron, J. Mol. Des. 5 (2006) 503.
[12] B. Debnath, S. Gayen, S. Samanta, A. Basu, B. Ghosh, T. Jha, Ind. J. Chem. A 45A (2006) 93–99.
[13] A. Basu, S. Gayen, S. Samanta, P. Panda, K. Srikanth, T. Jha, Can. J. Chem. 84 (2006) 458–463.
[14] Chem 3D Pro Version 5.0 and Chem Draw Ultra Version 5.0 are programs, CambridgeSoft Corporation, U.S.A., 1999.
[15] R. Franke, The Theoretical Drug Design Methods, Elsevier, Amsterdam, 1984.
[16] G.W. Snedecor, W.G. Cochran, Statistical Methods, Oxford & IBH, New Delhi, 1967.
[17] H. Kubinyi, QSAR: Hansch Analysis and Related Approaches, VCH, New York, 1993.
[18] L. Eriksson, J. Jaworska, A.P. Worth, M.T.D. Cronin, R.M. McDowell, P. Gramatica, Environ. Health Perspect. 111 (2003) 1361–1375.